2013

Effects of feed and draw solution temperature and transmembrane temperature difference on the rejection of trace organic contaminants by forward osmosis

Ming Xie
University of Wollongong, mx504@uowmail.edu.au

William E. Price
University of Wollongong, wprice@uow.edu.au

Long D. Nghiem
University of Wollongong, longn@uow.edu.au

Menachem Elimelech
Yale University

Publication Details

Xie, M., Price, W. E., Nghiem, L. D. & Elimelech, M. (2013). Effects of feed and draw solution temperature and transmembrane temperature difference on the rejection of trace organic contaminants by forward osmosis. Journal of Membrane Science, 438 57-64.

Effects of feed and draw solution temperature and transmembrane temperature difference on the rejection of trace organic contaminants by forward osmosis

Abstract

The effects of feed and draw solution temperature and transmembrane temperature difference on the rejection of 12 trace organic contaminants (TrOCs) by two forward osmosis (FO) membranes were investigated. The membrane structure parameter (S) and the reverse salt (NaCl) flux selectivity (RSFS) were constant over the temperature range of 20-40 1C, suggesting that within this range, the solution temperature did not significantly influence the membrane polymeric structure. Draw solution properties, including diffusivity, viscosity, and osmotic pressure, played an important role in water and reverse salt (NaCl) flux behaviour and TrOC rejection. Pure water and salt (NaCl) permeability coefficients of the two forward osmosis membranes increased as both the feed and draw solution temperatures increased from 20 to 40 1C due to an increase in solute diffusivity and a decrease in water viscosity. Rejection of charged TrOCs was higher than that of neutral TrOCs and their rejection was insensitive to temperature variation. On the other hand, rejection of neutral TrOCs decreased significantly when the feed and draw solution temperatures were 40 and 20 1C, respectively, due to the increase in their diffusivity at an elevated temperature. By contrast, rejection of neutral TrOCs increased when the feed and draw solution temperatures were 20 and 40 1C, respectively. The reverse salt (NaCl) flux increased due to an increase in the draw solute diffusivity. In addition, at a higher draw solution temperature, the dilution effect induced by higher water flux and the hindrance effect enhanced by a higher reverse salt (NaCl) flux led to the increase in the rejection of neutral TrOCs.

Keywords

solution, draw, feed, effects, transmembrane, temperature, difference, osmosis, rejection, trace, forward, contaminants, organic

Disciplines

Engineering | Science and Technology Studies

Publication Details

Xie, M., Price, W. E., Nghiem, L. D. & Elimelech, M. (2013). Effects of feed and draw solution temperature and transmembrane temperature difference on the rejection of trace organic contaminants by forward osmosis. Journal of Membrane Science, 438 57-64.

Effects of feed and draw solution temperature and transmembrane temperature difference on the rejection of trace organic contaminants by forward osmosis

Fresh manuscript submitted to

Journal of Membrane Science

March 2013

Ming Xie [1], William E. Price [2], Long D. Nghiem [1,*], and Menachem Elimelech [3]

[1] Strategic Water Infrastructure Laboratory, School of Civil, Mining and Environmental Engineering, University of Wollongong, Wollongong, NSW 2522, Australia

[2] Strategic Water Infrastructure Laboratory, School of Chemistry, University of Wollongong, Wollongong, NSW 2522, Australia

[3] Department of Chemical and Environmental Engineering, Yale University, New Haven, Connecticut 06520-8286, USA

---

* Corresponding author: Long Duc Nghiem, Email: longn@uow.edu.au; Ph +61 2 4221 4590

Abstract

The effects of feed and draw solution temperature and transmembrane temperature difference on the rejection of 12 trace organic contaminants (TrOCs) by two forward osmosis (FO) membranes were investigated. The membrane structure parameter (*S*) and the reverse salt (NaCl) flux selectivity (*RSFS*) were constant over the temperature range of 20 to 40 °C, suggesting that within this range, the solution temperature did not significantly influence the membrane polymeric structure. Draw solution properties, including diffusivity, viscosity and osmotic pressure, played an important role in water and reverse salt (NaCl) flux behaviour and TrOC rejection. Pure water and salt (NaCl) permeability coefficients of the two forward osmosis membranes increased as both the feed and draw solution temperatures increased from 20 to 40 °C due to an increase in solute diffusivity and a decrease in water viscosity. Rejection of charged TrOCs was higher than that of neutral TrOCs and their rejection was insensitive to temperature variation. On the other hand, rejection of neutral TrOCs decreased significantly when the feed and draw solution temperatures were 40 and 20 °C, respectively, due to the increase in their diffusivity at an elevated temperature. By contrast, rejection of neutral TrOCs increased when the feed and draw solution temperatures were 20 and 40 °C, respectively. The reverse salt (NaCl) flux increased due to an increase in the draw solute diffusivity. In addition, at a higher draw solution temperature, the dilution effect induced by higher water flux and the hindrance effect enhanced by a higher reverse salt (NaCl) flux led to the increase in the rejection of neutral TrOCs.

Keywords: Forward osmosis; rejection; temperature; transmembrane temperature difference; trace organic contaminants (TrOCs).

1. Introduction

Water scarcity exacerbated by population growth, industrialization, and increasingly irregular weather patterns presents a major challenge to the sustainable development of mankind [1]. Extraction of clean water from unconventional sources, such as municipal wastewater, is arguably feasible from both technical and economic points of view [1-2]. These unconventional water sources require extensive treatment for the protection of public health. For example, trace organic contaminants (TrOCs) are ubiquitous in secondary treated effluent and sewage-impacted water bodies; ranging from a few nanograms per litre (ng/L) to several micrograms per litre (μg/L) [3-5]. Uncontrolled release of these TrOCs presents a threat to the aquatic environment, with effects such as acute and chronic toxicity to aquatic organisms, accumulation in the ecosystem and loss of habitats and biodiversity, as well as a range of possible adverse effects on human health. Numerous studies have been conducted to enhance the removal capacity of current treatment processes or develop new technologies for better removal of these TrOCs from domestic wastewater and other impaired water resources [2].

Forward osmosis (FO), a membrane-based separation technology, has received renewed attention in recent years [6-7]. In lieu of hydraulic pressure, FO utilizes a highly concentrated draw solution to induce the driving force for separation. The transport of water molecules is osmotically driven and contaminants in the feed solution can be rejected by the active layer of the FO membrane. When the draw solute can add value to the extracted water, the diluted draw solution can be directly consumed without any further treatment and FO can be applied as a stand alone process [8]. FO can also be applied in conjunction with a draw solution recovery process, such as reverse osmosis and thermal separation (e.g. conventional column distillation [9-10] and membrane distillation (MD) [11-12]).

Temperature is an important factor governing mass transfer in membrane separation processes, including the FO process. In several practical applications of FO, there can be significant temporal and spatial variation in the temperature of feed solutions, such as secondary treated effluent or seawater. Similarly, draw solutions can be at higher temperatures than the feed solution as a result of thermal separation and recycling of the draw solution or using higher temperatures to increase the solubility of the draw solute. Such temperature variations could substantially impact the rejection of TrOCs by the FO process, as also observed in the NF and RO processes [13-14].

Several studies have examined the effect of temperature on the permeation of water [15-16] and inorganic salts [17] in the FO process. Generally, it was observed that water and salt permeabilities increased with increasing temperature in the FO process [16-20]. Recent studies have also focused on the impact of the temperature difference between the feed and draw solutions on water and draw solute permeation across FO membranes. Phuntsho et al. [17] examined the water flux behaviour with feed and draw solutions of different temperature and found that water flux increased significantly by increasing draw solution temperature. You et al. [15] proposed that the heat flux generated by the temperature difference between the feed and draw solutions could enhance the water flux due to the decrease in feed solution viscosity and the increase in water diffusivity. However, no studies to date have investigated the effect of temperature and temperature difference between feed and draw solutions on the rejection of contaminants in the feed solution, which is a critical aspect to the deployment of the FO process in wastewater reclamation. Elucidating the impact of temperature on the FO process can be useful for the management of thermal draw solution recovery processes, such as column distillation and MD, and optimization of FO performance with regard to solute rejection and water flux.

In this study, an asymmetric cellulose-based FO membrane and a thin-film composite polyamide FO membrane were used to investigate the rejection of 12 TrOCs under four feed and draw solution temperature combinations. Membrane intrinsic properties, namely pure water and salt (NaCl) permeability coefficients and membrane structural parameter, were determined to better elucidate the impact of temperature on water and reverse salt (NaCl) fluxes and TrOC rejection. The implications of the results for FO process performance and optimization are elucidated and discussed.

2. Materials and methods

2.1. Forward osmosis membranes

Two commercially available FO membranes were used in this study: an asymmetric cellulose triacetate FO membrane (CTA membrane) acquired from Hydration Technology Innovations (Albany, OR) and a thin-film composite polyamide FO membrane (TFC membrane) obtained from Oasys Water (Boston, MA). The CTA membrane has been the subject of numerous previous FO studies and is composed of a cellulose triacetate layer with an embedded woven support mesh [6, 21]. On the other hand, the TFC membrane is a

relatively new product. It is reported to have a thin selective polyamide active layer on top of a porous polysulfone support layer [22].

2.2. Forward osmosis system

A bench-scale cross-flow FO system was used (Supplementary Data, Figure S1). The membrane cell was made of acrylic plastic and had channel dimensions of 13 cm long, 9.5 cm wide, and 0.2 cm deep. The total effective membrane area was 123.5 cm^2. Two variable speed gear pumps (Micropump, Vancouver, WA) were used to circulate the feed and draw solutions. Flow rates of the feed and draw solutions were monitored using rotameters and kept constant at 1 L/min (corresponding to a cross flow velocity of 9 cm/s). The draw solution reservoir was placed on a digital balance (Mettler Toledo Inc., Hightstown, NJ) and weight changes were recorded by a computer to calculate the permeate water flux. The conductivity of the draw solution (0.5 M NaCl) was continuously measured using a conductivity probe with a cell constant of 1/cm (Cole-Parmer, Vernon Hills, IL). To maintain constant draw solution concentration, a peristaltic pump was regulated by a conductivity controller to intermittently dose a small volume of a concentrated draw solution (6 M NaCl) into the draw solution reservoir (control accuracy was ± 0.1 mS/cm). The concentrated draw solution makeup reservoir was also placed on the same digital balance. This setup ensured that the transfer of liquid between the two reservoirs did not interfere with the measurement of permeate water flux and that the system could be operated at a constant osmotic pressure driving force during the experiment. Details about the design and operation of this FO system are available elsewhere [23].

2.3. Membrane characterisation

Changes in key properties of the two membranes, including pure water permeability coefficient A, salt (NaCl) permeability coefficient B, and membrane structural parameter of support layer S at different feed and draw solution temperatures were determined using the standard experimental procedure recently proposed by Cath et al. [24]. Briefly, pure water and salt permeability coefficients were measured using deionized water and 2000 mg/L NaCl, respectively. The cross-flow RO filtration system used for this measurement has been described in details elsewhere [23]. Experiments were conducted at 20 ± 0.1 °C and 40 ± 0.1 °C. The cross-flow velocity was maintained at 25 cm/s. Prior to each measurement, the membranes were compacted at 15 bar with deionised water for at least 12 hours until the permeate water flux had been stabilized. The pure water permeability coefficient was

measured at 10 bar (or 145 psi). NaCl was then added to the feed solution at a concentration of 2000 mg/L to determine the salt (NaCl) permeability coefficient at 10 bar (or 145 psi). The RO system was stabilised for 2 hours before recording permeate water flux with 2000 mg/L NaCl solution, J_W^{NaCl} , and taking feed and permeate samples to determine the observed NaCl rejection, R_o.

The water permeability coefficient, *A,* was determined by dividing the pure water permeate flux (J_w^{RO}) by the applied hydraulic pressure, ΔP:

$$A = J_w^{RO} / \Delta P \qquad (1)$$

The observed salt (NaCl) rejection, R_o, was calculated from the difference between the bulk feed (c_b) and permeate (c_p) salt concentrations, $R_o = 1 - c_p/c_b$, and then the salt (NaCl) permeability coefficient, *B*, was determined from [25-26]:

$$B = J_w^{NaCl}\left(\frac{1-R_o}{R_o}\right)\exp\left(-\frac{J_w^{NaCl}}{k_f}\right) \qquad (2)$$

where k_f is the mass transfer coefficient for the crossflow channel of the RO membrane cell.

The mass transfer coefficient (k_f) was experimentally determined using a protocol described in our previous publication [23]. Using the permeate and feed salt concentrations (and thus, the corresponding osmotic pressures based on the van't Hoff equation, π_p and π_b, respectively), the applied pressure (ΔP), the pure water flux (J_w), and the permeate flux with the 2000 mg/L NaCl solution (J_{salt}) enables the evaluation of the salt concentration at the membrane surface. This membrane surface concentration is used in the film model for concentration polarization to determine the mass transfer coefficient k_f [27]:

$$k_f = \frac{J_{salt}}{\ln\left[\frac{\Delta P}{\pi_b - \pi_p}\left(1 - \frac{J_{salt}}{J_w}\right)\right]} \qquad (3)$$

The membrane structural parameter of support layer *S* was evaluated in the bench-scale cross-flow FO system described in section 2.2. The water flux, J_w^{FO} , using a 0.5 M NaCl draw solution and deionized water feed solution was measured with the membrane in FO mode (i.e., active layer facing the feed solution) under four different feed and draw solution temperature scenarios (i.e., feed and draw solution temperatures of 20 °C and 20 °C;

145 40 °C and 40 °C; 40 °C and 20 °C; and 20 °C and 40 °C). The membrane structural
146 parameter *S* was determined using [28]:

147 $$S = \frac{D_s}{J_w^{FO}} \ln\left(\frac{B + A\pi_{D,b}}{B + J_w + A\pi_{F,m}} \right) \quad (4)$$

148 where D_s is the bulk solution diffusivity of the draw solute, $\pi_{D,b}$ is the bulk osmotic pressure
149 of the draw solution, and $\pi_{F,m}$ is the osmotic pressure at the membrane surface on the feed
150 side (zero for deionized water feed). *A* and *B* in Eq. 4 were calculated using Eqs. 1 and 2.

151 Reverse salt flux selectivity (*RSFS*) is defined as the ratio of water flux, J_w^{FO}, to
152 reverse salt (NaCl) flux, J_s^{FO}, in the FO process. The *RSFS* is independent of the membrane
153 support layer properties and can quantitatively describe the FO membrane performance [29]:

154 $$RSFS = \frac{A}{B} nRT \quad (5)$$

155 where *n* is number of dissolved species created by the draw solute (2 for NaCl), *T* is the draw
156 solution temperature, and *R* is the ideal gas constant.

157 ## *2.4. Model trace organic contaminants*

158 A total of 12 TrOCs, including nine pharmaceuticals and personal care products, and
159 three pesticides, were selected for this investigation (Table 1). These TrOCs are frequently
160 detected in secondary treated effluent and sewage-impacted water bodies at trace levels. They
161 were also selected to represent a diverse range of physicochemical properties (e.g., charge,
162 hydrophobicity, and molecular weight). The model TrOCs are small molecular weight
163 compounds (less than 362 g/mol) with effective hydrophobicity measured by distribution
164 coefficient (log *D*) at neutral pH in the range from -0.96 to 5.28. The TrOCs were purchased
165 as analytical grade standards. A combined stock solution containing 1 g/L of each compound
166 was prepared in pure methanol. The stock solution was kept at −18 °C in the dark and was
167 used within one month.

168 **Table 1:** Key physicochemical properties of selected trace organic contaminants (TrOCs).

Compound	Category	Molecular weight (g/mol)	Log *D* [a] (pH 7)	pK_a [a]	Diffusion coefficient [b] ($\times 10^{-6}$ cm^2/s)	
					20°C	40°C
Amitriptyline	Hydrophilic,	277	2.28	9.18	4.82	7.83

Trimethoprim	charged	290	0.27	7.04	4.99	8.11
Sulfamethoxazole		253	-0.96	5.18	5.99	9.73
Diclofenac		296	1.77	4.18	5.24	8.52
Bezafibrate		362	-0.93	3.29	4.45	7.23
Caffeine	Hydrophilic, neutral	194	-0.63	0.52	7.23	11.75
Atrazine		216	2.64	2.27	5.75	9.34
Primidone		218	0.83	12.26	5.98	9.71
Carbamazepine		236	1.89	13.94	5.84	9.49
Pentachlorophenol		266	2.85	4.68	6.72	10.92
Linuron	Hydrophobic, neutral	249	3.12	12.13	5.9	9.58
Triclosan		290	5.28	7.8	5.58	9.06

[a] Values for pK_a and log D were obtained from the SciFinder Scholar (ACS) database

[b] Calculated using USEPA On-line Tools - "Estimated Diffusion Coefficients in Air and Water" (http://www.epa.gov/athens/learn2model/part-two/onsite/estdiffusion.html)

2.5. Trace organic contaminant rejection experiments

The TrOCs stock solution was added to a background electrolyte solution (20 mM NaCl and 1 mM $NaHCO_3$) to obtain a feed solution concentration of 2 μg/L. Either HCl (1 M) or NaOH (1 M) was introduced to the feed tank to adjust the initial pH value of the feed solution. A draw solution of 0.5 M NaCl was prepared in Milli-Q water in a volumetric flask.

Trace organic contaminant rejection experiments were conducted in the FO mode where the active layer of the membrane faced the feed solution. The initial volumes of the feed and draw solutions were 4 L and 1 L, respectively. Feed and draw solution tanks and pipelines were covered by thermal insulation foam to minimize the water evaporation loss and heat loss. A new FO membrane coupon was used for each experiment. The experiment was concluded when 1 L water permeated through the membrane (i.e., 25% water recovery). Volumes of feed and draw solutions were checked and compared with water flux data at the conclusion of each experiment to make sure that water evaporation from the feed and draw solution tanks was negligible (the difference between measured volume and water flux data less than 3%). Samples from both the feed and draw solutions were collected at the beginning and after 1 L of water had permeated through the FO membrane for solid phase extraction (SPE) and subsequent LC-MS analysis.

TrOC rejection is calculated by taking into account the dilution of the draw solution using a mass balance calculation. A dilution factor (*DF*) is introduced to calculate the concentration of TrOCs in the permeate sample, which is defined as

$$DF = \frac{V_{ds,f}}{V_p} \quad (6)$$

where $V_{ds,f}$ is the final volume of the draw solution and V_p is the volume of permeate. The TrOC rejection, R (%), is calculated from

$$R = \left(1 - \frac{DF \times C_{ds,f}}{C_{f,0}}\right) \times 100 \quad (7)$$

Here, DF is the dilution factor obtained from Eq. 6, $C_{ds,f}$ is the final draw solution concentration of the TrOC, and $C_{f,0}$ is the initial feed concentration of the TrOC.

2.6. Analytical methods

The feed and draw solution samples were extracted using Oasis HLB cartridges (Waters, Milford, MA, USA) prior to LC-MS analysis to determine the concentration of TrOCs. The cartridges were pre-conditioned with 7 mL dichloromethane and methanol (1:1, v/v), 7 mL methanol, and 7 mL reagent water. The sample was 500 mL in volume and was first adjusted to pH 2 – 3 and then loaded onto the cartridges at a flow rate of approximately 2 mL/min. The cartridges were then rinsed with 20 mL of Milli-Q water and dried with a gentle stream of high purity nitrogen for 30 min. The TrOCs were eluted from the cartridges using 7 mL methanol followed by 7 mL dichloromethane and methanol (1:1, v/v) at about 2 mL/min. The eluted samples were evaporated to dryness in a water bath at 40 °C for two to three hours under a gentle stream of high purity nitrogen gas. The extracted residues were then redissolved in 200 µL methanol solution containing 5 µg carbamazepine- d_{10} and transferred into 2 mL vials for LC-MS analysis.

Analyses of the trace organic contaminants were conducted using a Shimadzu LC-MS system (LC-MS 2020) equipped with an electrospray ionization (ESI) interface. A Phenomenex Kinetex 2.6 µm C8 column (50 mm × 4.6 mm) was used as the chromatography column and was maintained at 26 °C inside a column oven (CTO-20A). The mobile phase was Milli-Q water buffered with 0.1% (v/v) formic acid and acetonitrile. The details about the gradient elution are provided in Supplementary Data Table S1. The mobile phase flow rate was 0.5 mL/min and the sample injection volume was 10 µL. The analytes from the HPLC system were fed directly into a quadrupole mass spectrometer via an ESI source. ESI positive ionization $[M+H]^+$ mode was adopted for caffeine, primidone, trimethoprim, sulfamethoxazole, carbamazepine, bezafibrate, atrazine, linuron and amitriptyline while ESI

negative ionization $[M-H]^-$ mode was used for pentachlorophenol, diclofenac and triclosan. All mass spectra were acquired in selective ion monitoring mode with the detector voltage of 0.9 kV, desolvation line temperature of 250 °C, and heating block temperature of 200 °C. High purity nitrogen was used as both the nebulizing and drying gas at a flowrate of 1.5 and 10 L/min, respectively. Standard solutions of the analytes were prepared at 1, 10, 50, 100, 500 and 1000 ng/mL, and an internal instrument calibration was carried out with carbamazepine-d_{10} as the internal standard. The calibration curves for all the analytes had a correlation coefficient of 0.99 or higher.

3. Results and discussion

3.1. Membrane properties

The *A* and *B* values (i.e. pure water and salt (NaCl) permeability coefficients) of both the CTA and TFC membranes increased with an increase in feed solution temperature (Table 2). Results reported here are consistent with a previous study conducted by Wong et al. [30] and can be attributed to an increase in solute diffusivity and a decrease in viscosity of water as the temperature increases. While the *A* and *B* values of the TFC membrane were substantially different from those of the CTA membrane, their responses to temperature variation are similar. It is noteworthy that the membrane structural parameter *S* was largely unchanged when the temperature of both the feed and draw solutions increased from 20 to 40 °C (Figure 1). This finding indicates that the membrane polymer structure does not change when solution temperature increases from 20 to 40 °C. Similarly, no statistically significant changes in the *S* value of the two membranes could be observed when the feed and draw solution temperatures were 40 and 20 °C, respectively. The p-values of the one-sample t-test on the structural parameter *S* of the CTA and TFC membranes (n=4) were 0.08 and 0.07, respectively. In addition, the calculation of the *S* value using Eq. 4 can result in some inherent error when temperatures of feed and draw solutions are different [30]. Because there was heat transfer induced by the temperature difference between the feed and draw solution, the *A* and *B* values of the membrane active layer were likely not the same as the values used in Eq. 4, which were obtained from RO experiments at the same feed solution temperature.

Table 2: Water and salt (NaCl) permeability coefficients of CTA and TFC FO membranes at different temperatures (mean value ± standard deviation from two membrane samples).

Temperature	Membrane	Water permeability	Salt (NaCl) permeability

(°C)		coefficient, *A* ($\times 10^{-12}$ m/s·Pa)	coefficient, *B* ($\times 10^{-8}$ m/s)
20	CTA	1.81 ± 0.27	6.81 ± 0.11
40		1.94 ± 0.09	9.92 ± 0.25
20	TFC	13.1 ± 0.07	4.56 ± 0.37
40		21.7 ± 0.31	8.06 ± 0.14

252 **Table 3**: Key properties of the 0.5 M NaCl draw solution.

Thermodynamic property	Unit	Temperature (°C)	
		20	40
Osmotic pressure [a]	bar	24.05	25.69
Viscosity [39]	μPa·s	1043.2	684.8
Diffusion coefficient [40]	$\times 10^{-9}$ m^2/s	1.2	2.51

253 [a] Calculated using OLI Stream Analyser (OLI Systems, Inc., Morris Plains, NJ

254

255

256

257

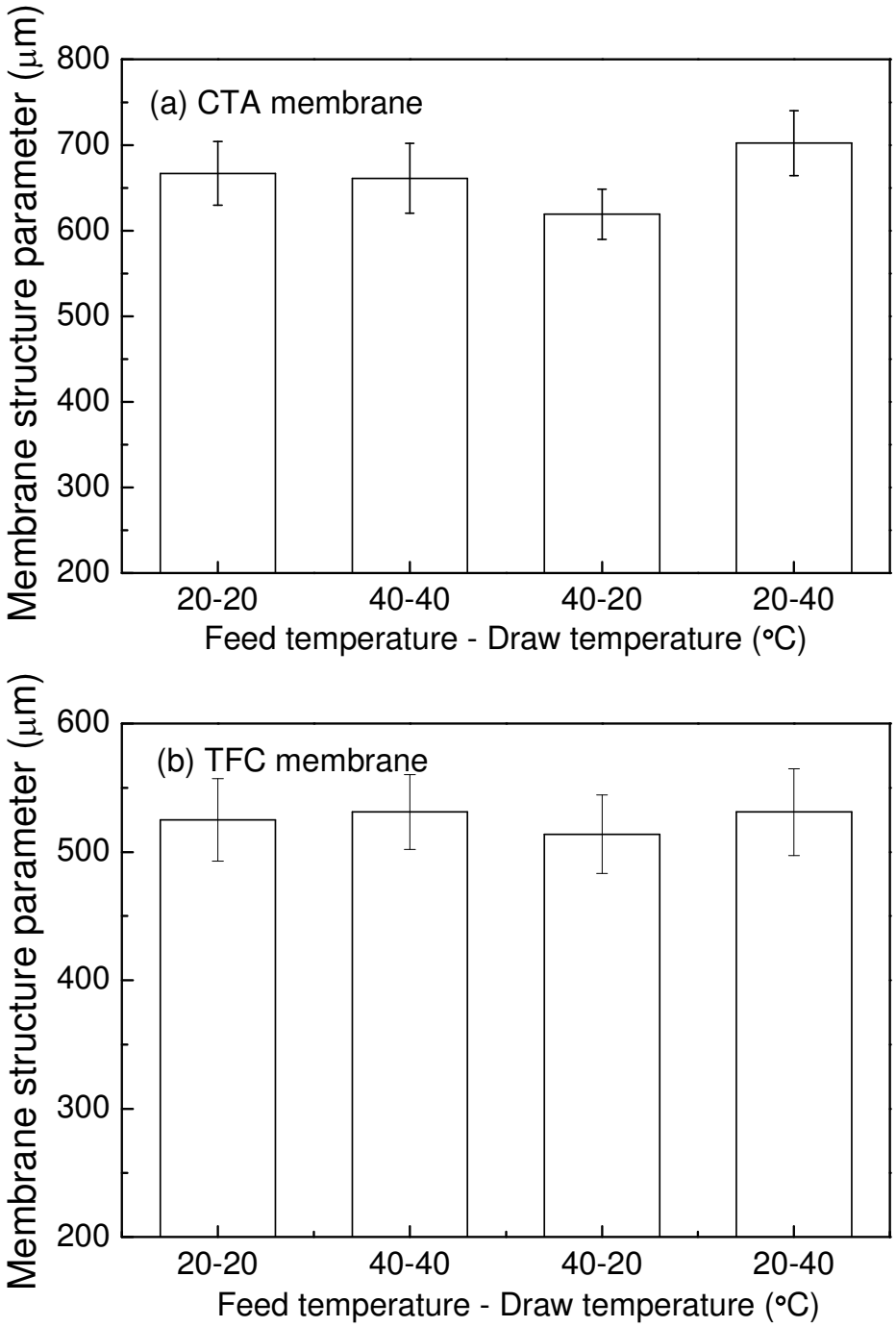

258

259 **Figure 1:** Membrane support layer structural parameter for (a) CTA and (b) TFC membranes
260 at varying feed and draw solution temperatures. Experimental conditions were as follows: FO
261 mode (i.e. feed solution facing membrane active layer), deionized water as feed solution,
262 draw solution = 0.5 M NaCl, and cross-flow rate = 1 L/min for both sides (corresponding to
263 cross flow velocity = 9 cm/s). Four different feed and draw solution temperature scenarios
264 were used: under the condition of same feed and draw solution temperature at 20 and 40 °C;
265 under the conditions of feed temperature at 40 °C and draw solution temperature at 20 °C,

and feed temperature at 20 °C and draw solution temperature at 40 °C. Error bars represent standard deviation of data obtained from two repeated experiments.

3.2. Water and reverse salt (NaCl) fluxes

Both water and reverse salt (NaCl) fluxes were significantly impacted by feed and draw solution temperatures (Figure 2). When the feed and draw solution temperatures were the same (denoted 20-20 and 40-40 in Figure 2), the water and reverse salt (NaCl) fluxes of the CTA and TFC membranes substantially increased as the solution temperature increased from 20 to 40°C. This observation is in good agreement with the increase in the membrane *A* and *B* values reported in Section 3.1 and the literature [17, 31].

In addition to the isothermal conditions investigated by these two previous studies [17, 31], the effects of transmembrane temperature difference between the feed and draw solutions on solute and water transport were also examined in the current study. Water and reverse salt (NaCl) fluxes of both membranes increased slightly when either the feed or draw solution temperature increased to 40 °C and the other remained at 20 °C (denoted 40-20 and 20-40 in Figure 2) compared to the isothermal condition where the feed and draw solution temperatures were both at 20 °C. The increase in feed solution temperature from 20 to 40 °C enhanced the diffusivity of water molecules, thereby increasing the water and reverse salt (NaCl) fluxes. On the other hand, the increase of draw solution temperature from 20 to 40 °C decreased draw solution viscosity and increased the draw solute diffusivity (Table 3), thereby increasing the water and reverse salt (NaCl) fluxes.

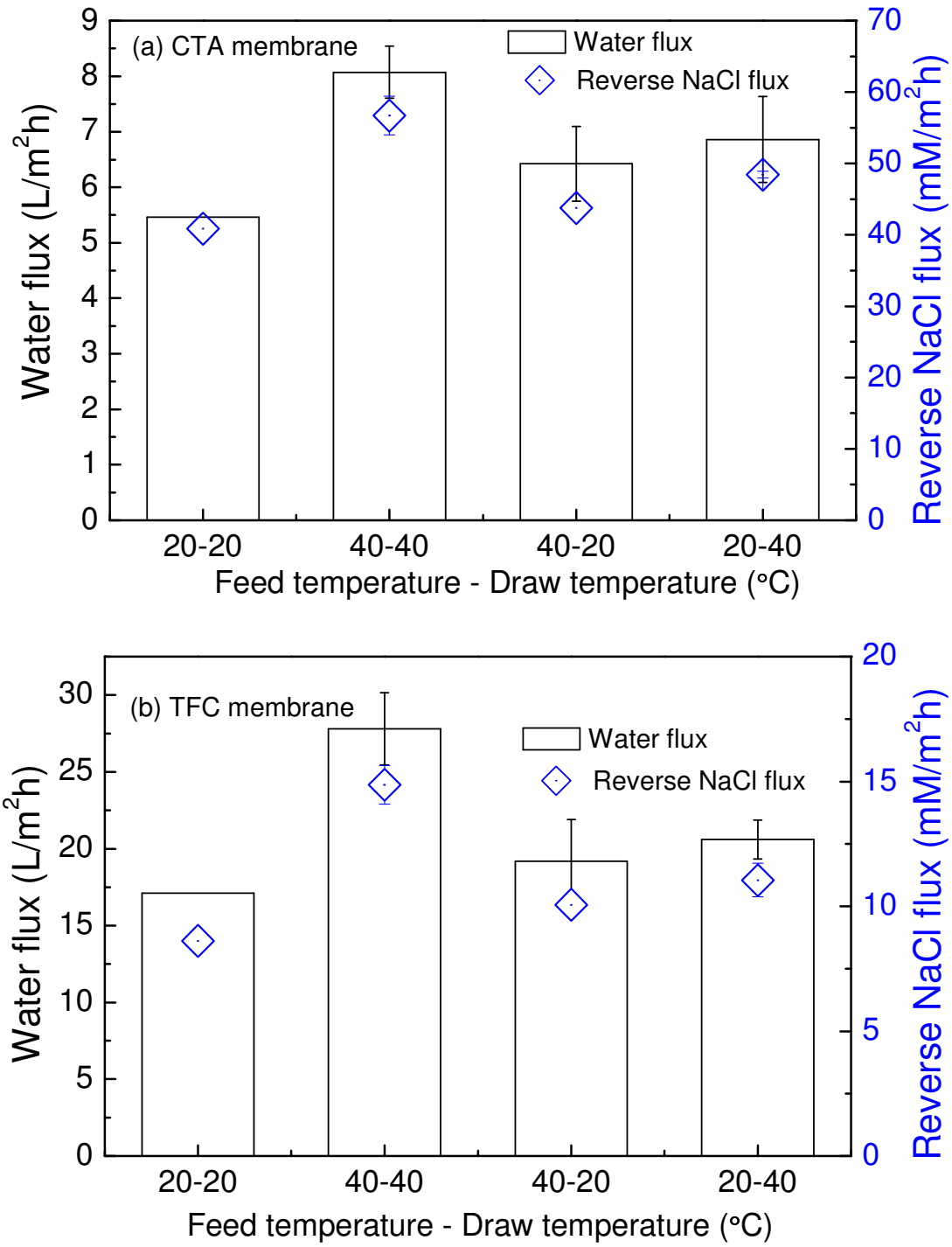

287

288 **Figure 2**: Water and reverse NaCl fluxes of (a) CTA and (b) TFC membranes at varying feed
289 and draw solution temperatures. Experimental conditions were described in Figure 1.

290

291 It is noteworthy that there was no discernible variation in the *RSFS* value of either
292 membrane regardless of the feed or draw solution temperatures (Figure 3). In addition, the
293 determined *RSFS* values obtained from the FO experiments (symbols) are almost identical to

those calculated from the intrinsic properties of the membranes (dashed line). The *RSFS* was independent of the membrane support layer properties and reflected the polymer structure of the membrane active layer. As a result, the insignificant variation in *RSFS* and the membrane *S* value (section 3.1) suggests that the membrane polymer structure did not change significantly within the temperature range of 20 to 40 °C. The water and reverse salt (NaCl) fluxes behaviour at different feed and draw solution temperature conditions was attributed mostly to the temperature-dependent properties of feed and draw solutions.

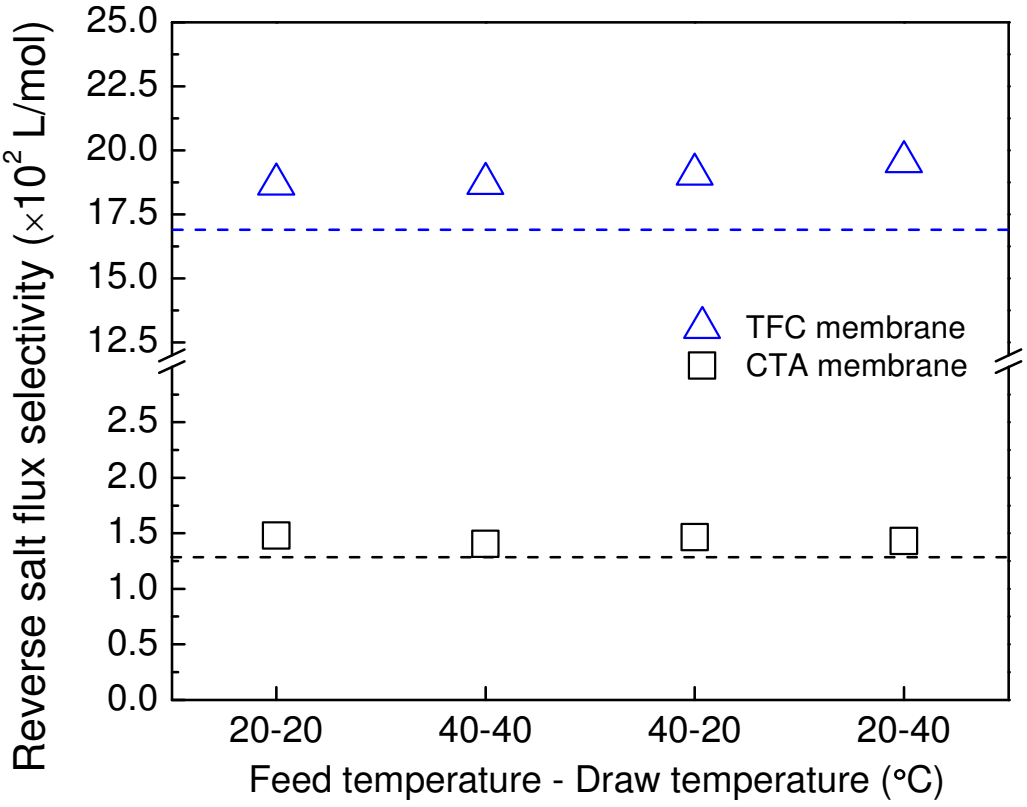

3.3. TrOC rejection performance

Overall, TrOC rejections by the TFC membrane were considerably higher than those by the CTA membrane. This can be attributed to the intrinsic properties of the TFC and CTA membranes. The TFC membrane has a smaller *B* value (Table 2) and higher *RSFS* value than the CTA membrane (Figures 3). Nevertheless, with respect to the rejection of TrOCs, both the CTA and TFC membranes responded to the variation in temperature and transmembrane temperature difference in a similar manner (Figure 4).

Figure 4: Rejections of 12 model TrOCs by the (a) CTA and (b) TFC FO membranes at varying feed and draw solution temperatures. The experimental conditions were as follows: FO mode (i.e. feed solution facing membrane active layer), initial concentrations of 12 trace

organic contaminants in the feed = 2 μg/L, pH = 7, background electrolyte contained 20 mM NaCl and 1 mM $NaHCO_3$, draw solution = 0.5 M NaCl, and cross flow rate = 1 L/min for both sides (corresponding to cross flow velocity = 9 cm/s). Four different feed and draw solution temperature scenarios were used: under the condition of same feed and draw solution temperature at 20 and 40 °C (denoted as F40-D40 and F20-D20); under the conditions of feed temperature at 40 °C and draw solution temperature at 20 °C (denoted as F40-D20), and feed temperature at 20 °C and draw solution temperature at 40 °C (denoted as F20-D40). Error bars represent standard deviation of four measurements in two repeated experiments.The rejection behaviours of charged and neutral TrOCs (Table 1) significantly differ from each other (Figure 4). In an aqueous solution, charged TrOCs are hydrated and the hydration of charged TrOCs significantly increases their apparent molecular sizes [32]. In addition, at the experimental pH value used in this study (pH 6.5), the CTA and TFC membranes are both negatively charged and electrostatic interaction is an important rejection mechanism of charged solutes [33-34]. Thus, rejections of charged TrOCs were notably higher than those of neutral TrOCs.

Temperature and transmembrane temperature difference only exerted a small influence on the rejection of charged TrOCs by the CTA and TFC membranes (Figure 4). By contrast, while rejection of both hydrophobic and hydrophilic neutral TrOCs increased with their molecular weight, their rejections varied significantly depending on the feed and draw solution temperatures. Results reported here demonstrate an intricate relationship between rejection of neutral TrOCs and temperature-dependent solvent and solute properties, such as solution viscosity and solute diffusivity. Overall, rejection of neutral TrOCs increased in the following order of feed and draw solution temperatures (in °C): 40 – 40 < 40 – 20 < 20 – 20 < 20 – 40.

When the feed and draw solution temperatures are the same, the low rejection of neutral TrOCs at high solution temperature can be attributed to an increase in solute partition into the membrane and diffusion coefficient. The permeation of neutral TrOCs is governed by "solution-diffusion" mechanism [35-36], where TrOCs first partition into the membrane active layer and then diffuse through it. The diffusion of TrOCs can be described by Fick's law and it is proportional to the diffusion coefficient [37]. A higher solution temperature favoured the partition of hydrophobic neutral TrOCs into the membrane. Notably, the adsorbed amounts of linuron and triclosan (with their Log *D* values > 3) increased by one order of magnitude with the increase of feed solution temperature from 20 to 40 °C (Figure 5).

345 At the same time, the diffusion coefficients of neutral TrOCs increase significantly (Table 1),
346 thereby leading to a markedly decrease in their rejections (Figure 4).

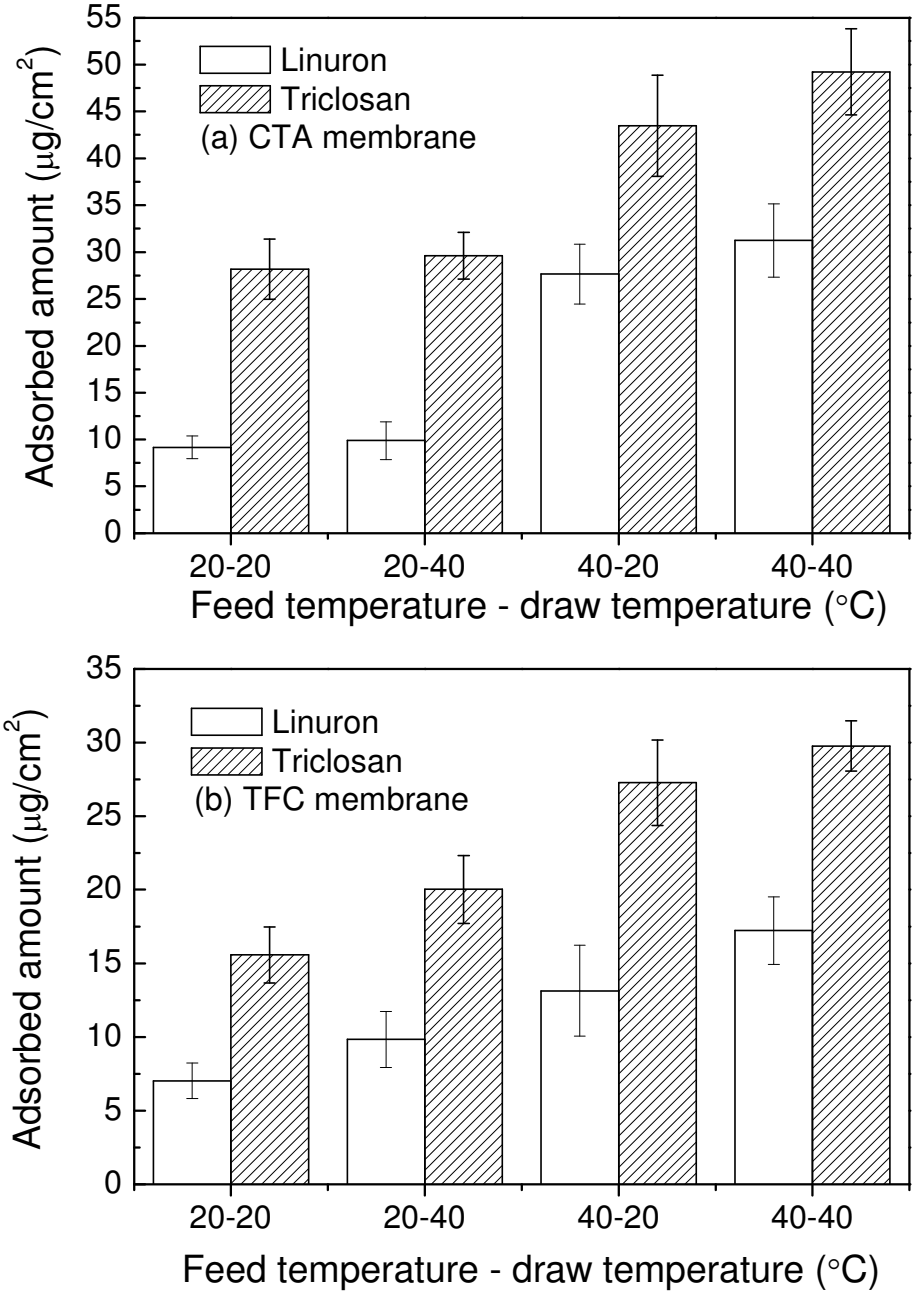

347

348 **Figure 5:** Adsorbed amount of linuron and triclosan by (a) CTA and (b) TFC membranes at
349 varying feed and draw solution temperatures. The adsorption amount was calculated using
350 mass balance. Experimental conditions were described in Figure 4.

351 Transmembrane temperature difference between the feed and draw solutions impacts
352 the water and reverse salt flux, which can subsequently influence the rejection of neutral
353 TrOCs. The diffusion coefficient of the draw solute increased with the increase in draw

solution temperature, resulting in an increase in both the water and reverse salt flux (Figure 2). Consequently, the increase in water flux can directly contribute to an increase in rejection, which is similar to that observed in the nanofiltration or reverse osmosis processes [38]. In addition, the increase in reverse salt flux can retard the forward diffusion of neutral TrOCs [23], thereby leading to higher rejection of these contaminants.

3.4. Implications for FO systems

The enhanced rejection of neutral TrOCs and improved water flux reported here have important implications for the integration of the FO process with a thermally-driven separation process, such as MD or conventional column distillation, for recovering the draw solutes. These results highlight the potential of FO for water production from reclaimed wastewater and other unconventional water sources that may be impaired with TrOCs. MD has been widely recognised as a potential draw solution recovery process [11-12]. In the MD process, solar thermal or low-grade heat can be utilised to increase the feed solution (i.e. the diluted draw solution of the FO process) temperature for the extraction of water vapour across a microporous membrane which is condensed to the liquid form. Thus, integrating the MD process with FO can not only improve the water flux and TrOC rejection by FO process but also reduce the carbon footprint of the overall treatment system. Similarly, the enhanced performance at a high draw solution temperature can facilitate practical deployment of thermolytic salts, such as ammonium carbonate, as the draw solutes for FO [9-10].

4. Conclusions

Results reported here demonstrate that feed and draw solution temperature and transmembrane temperature difference have a significant impact on FO water and reverse salt (NaCl) fluxes as well as TrOC rejection. The membrane structural parameter (S) and the reverse salt flux selectivity ($RSFS$) did not change significantly in the temperature range of 20 to 40°C, indicating that any thermal-induced changes in the membrane polymer structure would be negligible. The increase in water and solute diffusivities at higher temperatures and the temperature-dependent draw solution properties governed the water and reverse salt (NaCl) flux behaviour and TrOC rejection. Because electrostatic interaction was an important rejection mechanism, rejection of charged TrOCs was higher than that of neutral TrOCs and their rejection was insensitive to temperature variation. Rejection of neutral TrOCs decreased significantly as the feed solution temperature increased from 20 to 40 °C. This decrease resulted from the enhanced diffusivity of neutral TrOCs at an elevated temperature. By

contrast, rejection of neutral TrOCs increased when the feed and draw solution temperatures were 20 and 40°C, respectively. This increase in the rejection of neutral TrOCs could be attributed to the changes in properties of the draw solution. Water flux enhanced by higher osmotic pressure led to a dilution effect. At the same time, an increase in the reverse salt (NaCl) caused by a higher draw solute diffusivity further hinder the forward diffusion of the neutral TrOCs from the feed to the draw solution.

5. Acknowledgments

The authors would like to thank Hydration Technology Innovations and Oasys Water for providing membrane samples. University of Wollongong is acknowledged for the provision of a doctoral scholarship to Ming Xie.

6. References

[1] M. Elimelech, W.A. Phillip, The Future of Seawater Desalination: Energy, Technology, and the Environment, Science, 333 (2011) 712-717.

[2] M.A. Shannon, P.W. Bohn, M. Elimelech, J.G. Georgiadis, B.J. Marinas, A.M. Mayes, Science and technology for water purification in the coming decades, Nature, 452 (2008) 301-310.

[3] T. Basile, A. Petrella, M. Petrella, G. Boghetich, V. Petruzzelli, S. Colasuonno, D. Petruzzelli, Review of Endocrine-Disrupting-Compound Removal Technologies in Water and Wastewater Treatment Plants: An EU Perspective, Industrial & Engineering Chemistry Research, 50 (2011) 8389-8401.

[4] M. Carballa, F. Omil, J.M. Lema, M.a. Llompart, C. García-Jares, I. Rodríguez, M. Gómez, T. Ternes, Behavior of pharmaceuticals, cosmetics and hormones in a sewage treatment plant, Water Research, 38 (2004) 2918-2926.

[5] S.A. Snyder, P. Westerhoff, Y. Yoon, D.L. Sedlak, Pharmaceuticals, Personal Care Products, and Endocrine Disruptors in Water: Implications for the Water Industry, Environmental Engineering Science, 20 (2003) 449-469.

[6] T.Y. Cath, A.E. Childress, M. Elimelech, Forward osmosis: Principles, applications, and recent developments, Journal of Membrane Science, 281 (2006) 70-87.

[7] S. Zhao, L. Zou, C.Y. Tang, D. Mulcahy, Recent developments in forward osmosis: Opportunities and challenges, Journal of Membrane Science, 396 (2012) 1-21.

[8] L.A. Hoover, W.A. Phillip, A. Tiraferri, N.Y. Yip, M. Elimelech, Forward with Osmosis: Emerging Applications for Greater Sustainability, Environmental Science & Technology, 45 (2011) 9824-9830.

[9] R.L. McGinnis, M. Elimelech, Energy requirements of ammonia–carbon dioxide forward osmosis desalination, Desalination, 207 (2007) 370-382.

[10] J.R. McCutcheon, R.L. McGinnis, M. Elimelech, A novel ammonia—carbon dioxide forward (direct) osmosis desalination process, Desalination, 174 (2005) 1-11.

[11] C.R. Martinetti, A.E. Childress, T.Y. Cath, High recovery of concentrated RO brines using forward osmosis and membrane distillation, Journal of Membrane Science, 331 (2009) 31-39.

[12] T.Y. Cath, D. Adams, A.E. Childress, Membrane contactor processes for wastewater reclamation in space: II. Combined direct osmosis, osmotic distillation, and membrane distillation for treatment of metabolic wastewater, Journal of Membrane Science, 257 (2005) 111-119.

[13] J.M. Arsuaga, M.J. López-Muñoz, J. Aguado, A. Sotto, Temperature, pH and concentration effects on retention and transport of organic pollutants across thin-film composite nanofiltration membranes, Desalination, 221 (2008) 253-258.

[14] R.R. Sharma, S. Chellam, Temperature and concentration effects on electrolyte transport across porous thin-film composite nanofiltration membranes: Pore transport mechanisms and energetics of permeation, Journal of Colloid and Interface Science, 298 (2006) 327-340.

[15] S.-J. You, X.-H. Wang, M. Zhong, Y.-J. Zhong, C. Yu, N.-Q. Ren, Temperature as a factor affecting transmembrane water flux in forward osmosis: Steady-state modeling and experimental validation, Chemical Engineering Journal, 198–199 (2012) 52-60.

[16] S. Zhao, L. Zou, Effects of working temperature on separation performance, membrane scaling and cleaning in forward osmosis desalination, Desalination, 278 (2011) 157-164.

[17] S. Phuntsho, S. Vigneswaran, J. Kandasamy, S. Hong, S. Lee, H.K. Shon, Influence of temperature and temperature difference in the performance of forward osmosis desalination process, Journal of Membrane Science, 415–416 (2012) 734-744.

[18] J.R. McCutcheon, M. Elimelech, Influence of concentrative and dilutive internal concentration polarization on flux behavior in forward osmosis, Journal of Membrane Science, 284 (2006) 237-247.

[19] B.S. Chanukya, S. Patil, N.K. Rastogi, Influence of concentration polarization on flux behavior in forward osmosis during desalination using ammonium bicarbonate, Desalination.

[20] C.A. Nayak, N.K. Rastogi, Forward osmosis for the concentration of anthocyanin from Garcinia indica Choisy, Separation and Purification Technology, 71 (2010) 144-151.

[21] J.R. McCutcheon, M. Elimelech, Influence of membrane support layer hydrophobicity on water flux in osmotically driven membrane processes, Journal of Membrane Science, 318 (2008) 458-466.

[22] N.Y. Yip, A. Tiraferri, W.A. Phillip, J.D. Schiffman, M. Elimelech, High Performance Thin-Film Composite Forward Osmosis Membrane, Environmental Science & Technology, 44 (2010) 3812-3818.

[23] M. Xie, L.D. Nghiem, W.E. Price, M. Elimelech, Comparison of the removal of hydrophobic trace organic contaminants by forward osmosis and reverse osmosis, Water Research, 46 (2012) 2683-2692.

[24] T.Y. Cath, M. Elimelech, J.R. McCutcheon, R.L. McGinnis, A. Achilli, D. Anastasio, A.R. Brady, A.E. Childress, I.V. Farr, N.T. Hancock, J. Lampi, L.D. Nghiem, M. Xie, N.Y. Yip, Standard Methodology for Evaluating Membrane Performance in Osmotically Driven Membrane Processes, Desalination, 312 (2013) 31-38.

[25] R.W. Baker, Membrane technology and applications, 2nd edition ed., John Wiley & Sons, Ltd, New York, NY, 2004.

[26] M. Mulder, Basic Principles of Membrane Technology, 2nd edition, 2nd edition ed., Kluwer Academic Publishers, Dordrecht, The Netherlands, 2001.

[27] I. Sutzkover, D. Hasson, R. Semiat, Simple technique for measuring the concentration polarization level in a reverse osmosis system, Desalination, 131 (2000) 117-127.

[28] S. Loeb, L. Titelman, E. Korngold, J. Freiman, Effect of porous support fabric on osmosis through a Loeb-Sourirajan type asymmetric membrane, Journal of Membrane Science, 129 (1997) 243-249.

[29] W.A. Phillip, J.S. Yong, M. Elimelech, Reverse Draw Solute Permeation in Forward Osmosis: Modeling and Experiments, Environmental Science & Technology, 44 (2010) 5170-5176.

[30] M.C.Y. Wong, K. Martinez, G.Z. Ramon, E.M.V. Hoek, Impacts of operating conditions and solution chemistry on osmotic membrane structure and performance, Desalination, 287 (2012) 340-349.

[31] J.R. McCutcheon, R.L. McGinnis, M. Elimelech, Desalination by ammonia-carbon dioxide forward osmosis: Influence of draw and feed solution concentrations on process performance, Journal of Membrane Science, 278 (2006) 114-123.

[32] L.D. Nghiem, A.I. Schafer, M. Elimelech, Role of electrostatic interactions in the retention of pharmaceutically active contaminants by a loose nanofiltration membrane, Journal of Membrane Science, 286 (2006) 52-59.

[33] M. Xie, W.E. Price, L.D. Nghiem, Rejection of pharmaceutically active compounds by forward osmosis: Role of solution pH and membrane orientation, Separation and Purification Technology, 93 (2012) 107-114.

[34] A.A. Alturki, J.A. McDonald, S.J. Khan, W.E. Price, L.D. Nghiem, M. Elimelech, Removal of trace organic contaminants by the forward osmosis process, Separation and Purification Technology, 103 (2013) 258-266.

[35] N.T. Hancock, W.A. Phillip, M. Elimelech, T.Y. Cath, Bidirectional Permeation of Electrolytes in Osmotically Driven Membrane Processes, Environmental Science & Technology, 45 (2011) 10642-10651.

[36] L.D. Nghiem, A.I. Schäfer, M. Elimelech, Nanofiltration of Hormone Mimicking Trace Organic Contaminants, Separation Science and Technology, 40 (2005) 2633-2649.

[37] E.L. Cussler, Diffusion mass transfer in fluid systems, 2009.

[38] L.D. Nghiem, A.I. Schäfer, M. Elimelech, Removal of Natural Hormones by Nanofiltration Membranes: Measurement, Modeling, and Mechanisms, Environmental Science & Technology, 38 (2004) 1888-1896.

[39] J. Kestin, H.E. Khalifa, R.J. Correia, Tables of the dynamic and kinematic viscosity of aqueous NaCl solutions in the temperature range 20--150 [degree]C and the pressure range 0.1--35 MPa, Journal of Physical and Chemical Reference Data, 10 (1981) 71-88.

[40] V.M.M. Lobo, Mutual diffusion coefficients in aqueous electrolyte solutions (Technical Report), Pure and Applied Chemistry, 65 (1993) 2613-2640.